Design of Nonuniform Metallic Anechoic Chamber for Radiation Pattern Measurement

Ali Farahbakhsh[1, *] and Mohammad Khalaj-Amirhosseini[2]

Abstract—Antenna pattern measurement is an essential step in antenna qualification which should be done in anechoic chambers. The common method for construction of the anechoic chamber is to cover all inside walls by the electromagnetic absorbers. In this paper, a new method is presented to design a fully metallic chamber by controlling the electromagnetic wave propagation inside the chamber and guiding them to a piece of absorber. Therefore, a desirable quiet zone is formed inside the chamber while a great reduction of absorber usage is achieved. The proposed chamber is analyzed using ray tracing method, and its performance is evaluated by simulation which shows the practicality of the proposed chamber.

1. INTRODUCTION

Anechoic chambers are presented in 1950 to satisfy the need of indoor antenna testing [1]. To surpass the reflection of electromagnetic (EM) waves and obtain quiet zone, all interior walls of the anechoic chamber are covered by the EM absorbers. Since the EM absorbers are not ideal and their absorption and working bandwidth are limited, the issue of anechoic chambers optimization has received increased interest, including minimization of absorber usage, chamber shaping and optimization of the absorber performance [2–13].

For instance, [4] utilizes the genetic algorithm and ray-tracing method to optimize the layout of ferrite tile absorber in a partially lined rectangular chamber to form a desirable quiet zone inside the chamber. Using the reported method, a reduction of 20% in absorber usage is achieved.

A number of reported methods increase the anechoic chamber performance by controlling the propagation of EM waves inside the chamber and force the absorbers to act with high performance [5]. In general, three major types of anechoic chambers are presented in the literatures, including rectangular [5], tapered [6] and double-horn [7, 8] chambers. Since the absorbers have a high reflection in low frequencies, the rectangular chambers are not suited for VHF/UHF band measurements; however they are the most used chamber type for antenna measurement. To overcome this problem, tapered and double-horn chambers are presented in which the absorbers reflection waves are controlled and a uniform illumination is formed across the quiet zone.

Recently, metallic ellipsoid and spherical anechoic chambers have been presented to reduce the absorber usage, in which the EM wave propagation is controlled inside the chamber and they are guided to a piece of EM absorber [12, 13].

Using a piece of absorber instead of covering all walls by the absorbers has some great benefits. In different frequency bands, the absorber piece can be easily changed and the optimum absorber for the desired frequency band can be used that leads to a wide band anechoic chamber. Also, antenna testing in clean room condition is desirable, but it is difficult to achieve clean room condition in traditional

[1] Electronic Engineering Department, Kerman Graduate University of Technology, Kerman, Iran. [2] Electronic Engineering Department, Iran University of Science and Technology, Tehran, Iran.

anechoic chambers due to air pollution of the classical carbon based absorbers. Since the absorbers on the chamber walls are omitted in the proposed chamber, a clean room condition is realizable inside it. In continuation of previous works and to improve them, this paper presents a nonuniform anechoic chamber structure which is smaller and needs fewer amount of EM absorber than the ellipsoid and spherical chambers.

2. DESIGN OF THE METALLIC CHAMBER

The structure of the proposed chamber is shown in Fig. 1. The source antenna is a standard horn antenna similar to the classical anechoic chambers and the source antenna is placed in the left side of the chamber. A proper piece of EM absorber is placed on the opposite side of the chamber and the quiet zone is assumed to be in the middle of the chamber and the Antenna Under Test (AUT) is placed in the quiet zone center. The chamber surface is metal and its shape is designed such that the EM waves are guided to the absorber after reflection from the chamber surface. The chamber shape cross-section in the polar system is determined by a super formula [14] that is given in (1) and the chamber shape is created by rotation of the cross-section around the x-axis.

$$r(\theta) = \left(\left| \frac{\cos\left(\frac{m\theta}{4}\right)}{a} \right|^{n_2} + \left| \frac{\sin\left(\frac{m\theta}{4}\right)}{b} \right|^{n_3} \right)^{-\frac{1}{n_1}} \qquad 0 \leq \theta \leq \pi \tag{1}$$

The super formula is introduced by Gielis in 2003 [14]. The super formula is a shape generator, and its special feature is that all natural shapes can be generated by changing only six coefficients (a, b, m, n_1, n_2, n_3). The enhanced Genetic Algorithm (GA) [15] is implemented to optimize the surface coefficients. The enhanced GA is employed to improve the efficiency of the GA using a fuzzy system to control GA parameters during running. The fitness of the chamber is calculated by software based on the Finite Element Method [16] and the quiet zone is evaluated using the VSWR method.
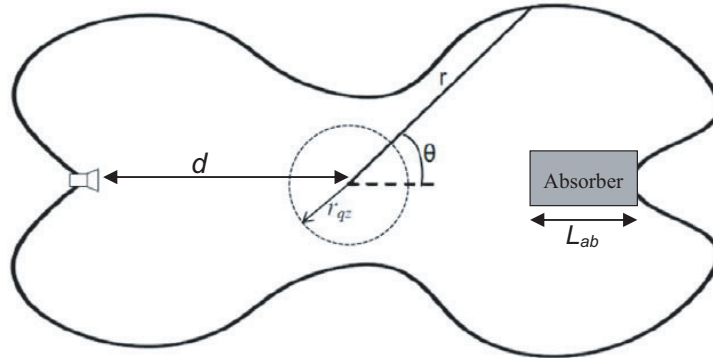
Figure 1. General structure of the metallic anechoic chamber.

3. QUIET ZONE PERFORMANCE

According to the definition, the quiet zone is a spherical volume inside the chamber, which only contains one wave front from the source antenna. The EM waves should be guided to the absorber after some reflections from the chamber surface without disturbing the quiet zone. Therefore, the design process is to find the chamber shape such that an acceptable quiet zone is formed inside the chamber while the chamber size is minimized.

The anechoic chamber performance is determined by the level of reflected EM waves from nearby objects inside the quiet zone. To evaluate the performance of the quiet zone, electric fields inside the quiet zone should be measured and then the Voltage Standing Wave Ratio of them is calculated as below [17, 18]:

$$VSWR = \frac{E_{\max}}{E_{\min}} \tag{2}$$

where $E_{\min}$ and $E_{\max}$ are the local minimum and maximum of the electric field amplitude on a straight line which is called calculation line. The reflectivity level (RL) is given below

$$\Gamma = 20 \cdot \log_{10} \frac{VSWR - 1}{VSWR + 1} \tag{3}$$

To take all reflection waves into account, the calculation line is rotated inside the quiet zone and the maximum RL in all directions is calculated as shown in Fig. 2.
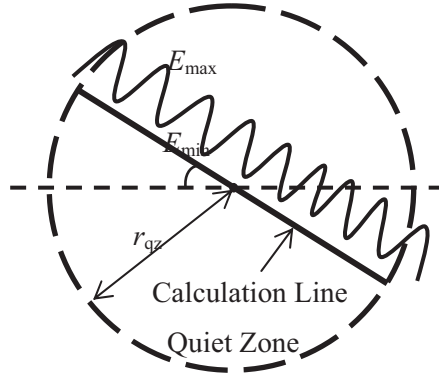
Figure 2. The maximum and minimum of the electric filed on a straight line is obtained to calculate the reflectivity level.

4. DESIGN PROCEDURE

In this section, a general method is proposed to optimally design a metallic anechoic chamber for antenna measurements. The design goal is to find the chamber shape such that a proper quiet zone is formed inside the chamber while the chamber size is minimized.

Therefore, the optimum values of the surface coefficients can be optioned through minimizing the following error function.

$$err = C_1 \cdot \max(\Gamma) + C_2 \cdot NCD \tag{4}$$

where NCD is the Normalized Chamber Dimension which is defined as the ratio of the maximum chamber dimension to the maximum acceptable chamber size. The variables C_1 and C_2 are the weighting coefficients. Also, the reflectivity level is calculated using VSWR method which is described in the previous section.

The enhanced GA is utilized to solve the above minimization problem. The electric fields inside the quiet zone are obtained by simulation using the COMSOL software [16] and from the simulation results, the error function is calculated.

In our work, the quiet zone radius (r_{qz}) is assumed to be $1\,\mathrm{m}$, and the required measuring distance (the distance between the source antenna and AUT) is $d = 2\,\mathrm{m}$.

Table 1 shows the optimum surface coefficients that obtained by the optimization algorithm. The optimum chamber shape and the trajectory of the EM rays inside the chamber are plotted in Fig. 3 using ray tracing method [19].

Table 1. Optimum surface coefficients.

Parameter	a	b	m	n_1	n_2	n_3
Value	5.74	1.66	3.93	81.43	53.08	22.897

As can be seen in Fig. 3, the radiated rays from the source are focused at a line on the opposite side of the chamber after reflection from the metallic surface. Therefore, all EM waves can be absorbed by putting a piece of EM absorber on the right side of the chamber.
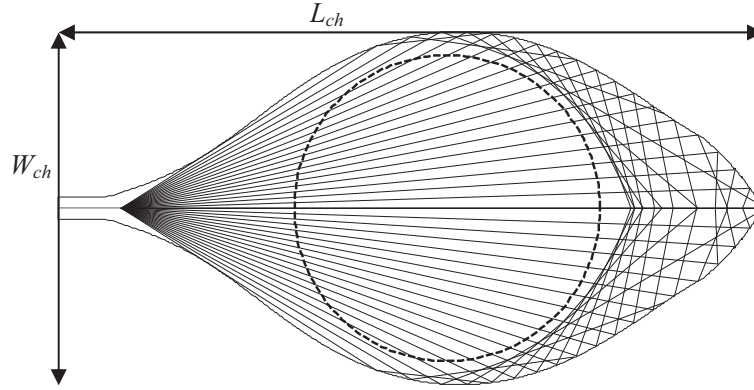
Figure 3. Cross-section of the metallic chamber and the trajectory of the EM rays inside it.

The optimum chamber will be scaled to achieve a chamber with different values of the quiet zone radius and the measuring distance according to following equations.

$$S_x = \frac{d}{2}, \quad S_y = r_{qz}, \quad S_x \geq S_y \tag{5}$$

where S_x and S_y are scaling coefficients in x and y directions, respectively. Variable d is the measuring distance, and r_{qz} is the quiet zone radius. Fig. 4 shows some chamber shapes according to different values of the scaling coefficients.
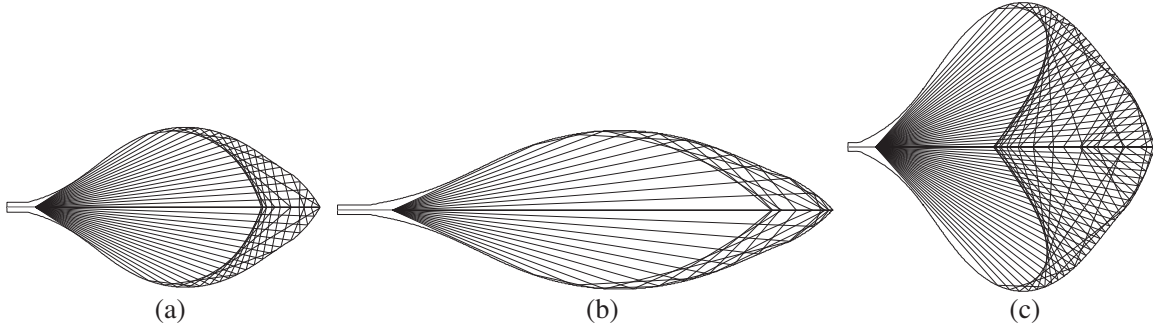
Figure 4. The chamber structure for different values of the scaling coefficients. (a) $S_x = 1$, $S_y = 1$, (b) $S_x = 2$, $S_y = 1$, (c) $S_x = 1$, $S_y = 2$.

Using Eq. (5) and the optimum surface coefficients, the chamber dimensions can be obtained as following.

$$L_{ch} = 3.44 \cdot S_x = 1.72 \cdot d \tag{6}$$
$$W_{ch} = 1.2 \cdot S_y = 2.4 \cdot r_{qz} \tag{7}$$

where L_{ch} and W_{ch} are length and width of the chamber, respectively.

All EM waves are absorbed by just using one piece of absorber. Therefore, it is possible to change absorber for different frequency bands and achieve a wide band anechoic chamber. A cylindrical absorber is used that is formed by putting some ordinary pyramid absorber around a metallic cylinder as shown in Fig. 5. The absorber length is

$$L_{ab} = 0.44\sqrt{S_x S_y} \tag{8}$$

The distribution of electric field inside the chamber is determined by a numerical simulation which is based on the Finite Element Method (FEM) [16]. The chamber electric fields for some frequencies are depicted in Fig. 6. Fig. 7 shows the maximum RL in all of the directions versus frequency. Observe that as expected, by increasing the operating frequency, the ray behavior of the EM waves becomes
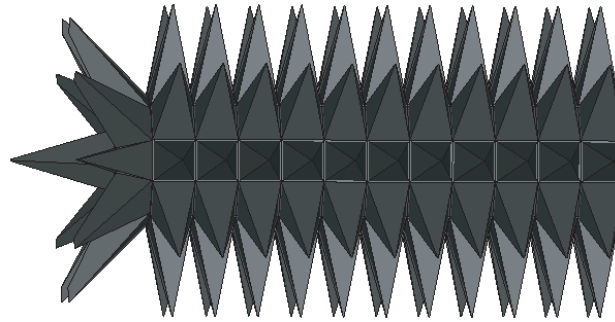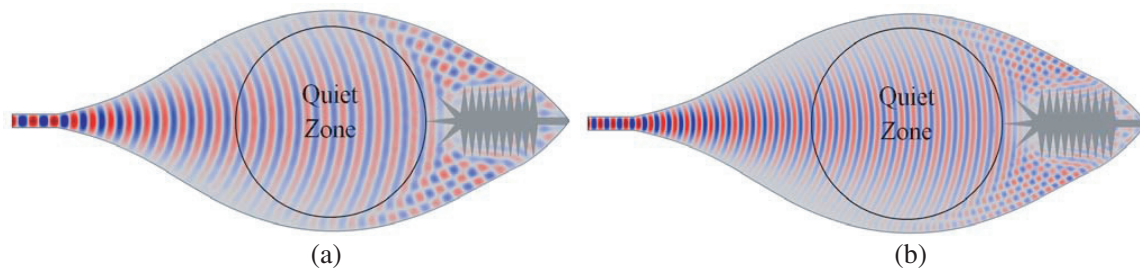
Figure 5. Cylindrical absorber.

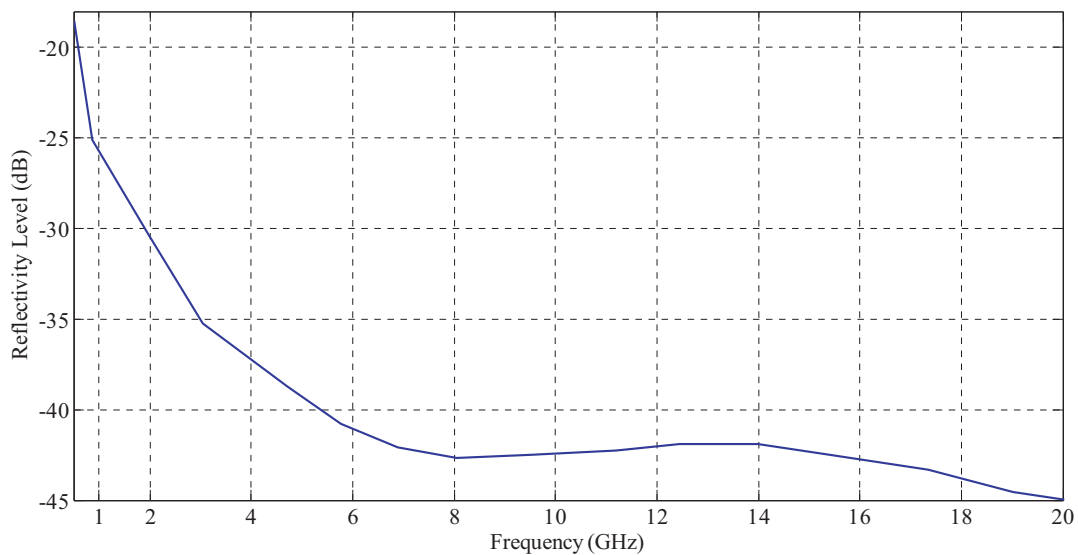**Figure 6.** Electric field distribution inside the chamber at (a) 3 GHz and (b) 5 GHz.

Figure 7. The maximum of the reflectivity level inside the quiet zone versus the operating frequency.

more visible and consequently the RL is decreased. From these results, one can find that the proposed chamber works well in the desired frequency range.

5. MECHANICAL IMPERFECTIONS

The mechanical accuracy in the manufacturing process of the proposed chamber specifies the chamber expense. Therefore, it is essential to investigate the effect of mechanical distortions on the chamber performance. To do this, a few amount of distortion in polar coordinate is applied to the chamber

surface as following.

$$r_{\text{distorted}} = r_{\text{distortion-free}} + \frac{\Delta}{2}\sin(N\theta) \qquad (9)$$

where $r_{\text{distorted}}$ and $r_{\text{distortion-free}}$ are the mathematical equations of the chamber surface in polar coordinate with and without distortion, respectively. Variable Δ is the distortion amount, and N determines the distortion form. Small and large values of N represent the chamber shape deformation and chamber surface roughness, respectively.

To study the effect of mechanical distortion, the quiet zone RL for different values of N and Δ is obtained using simulation and plotted in Fig. 8.
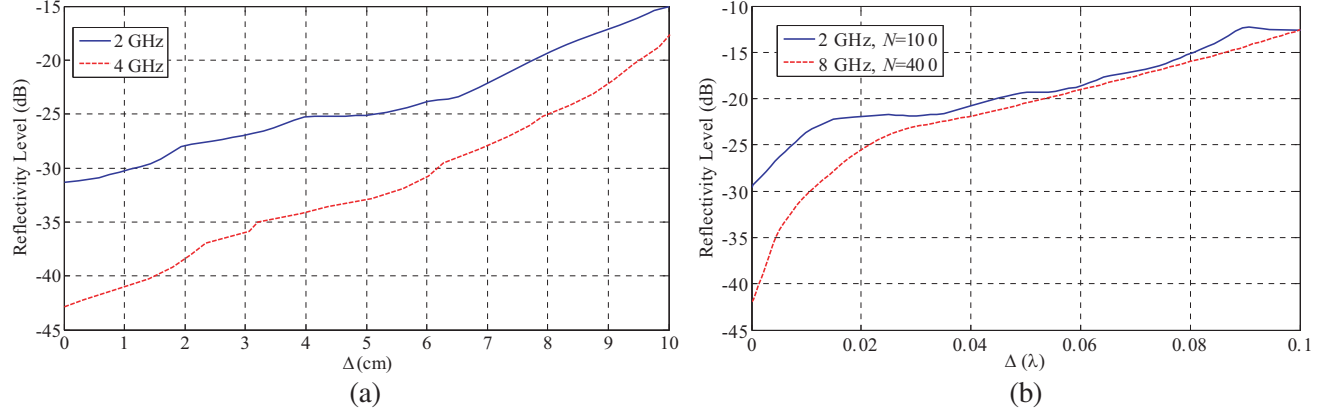
Figure 8. Effect of (a) the chamber shape deformation ($N = 3$) and (b) the chamber surface roughness ($N > 100$) on the quiet zone reflectivity level.

As can be seen, when the distortion amount is increased, the RL is disturbed slightly. But, the mechanical distortion does not have critical effects on the chamber performance and therefore, the proposed chamber can be manufactured using cheap methods and processes.
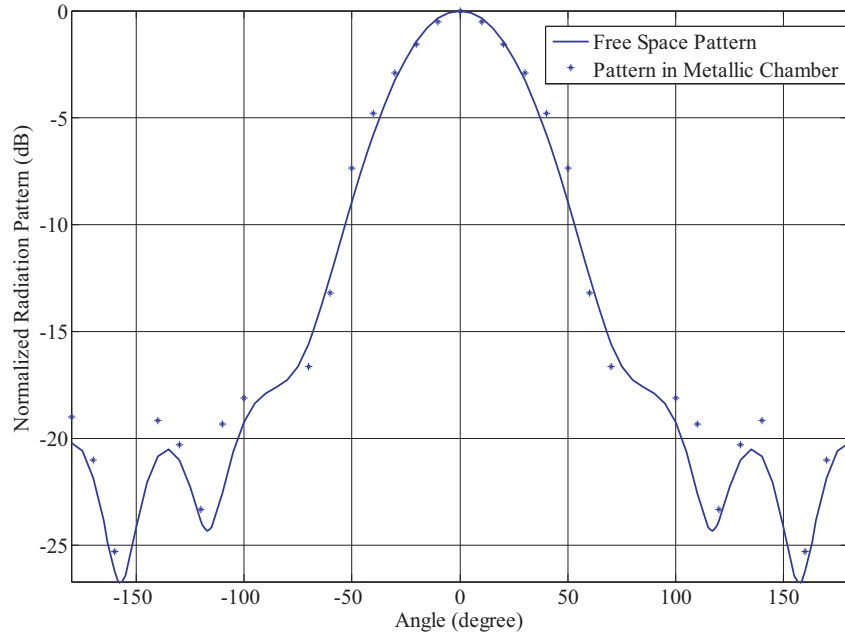
Figure 9. The normalized radiation patterns of a standard horn antenna inside the proposed chamber and in free space.

6. ANTENNA UNDER TEST SCATTERING

To investigate the effect of the AUT scattering, a standard 10 GHz horn antenna [20] is placed in the quiet zone center, and its radiation pattern is obtained using simulation results.

Figure 9 illustrates the AUT normalized radiation pattern in the E-plane, and as shown in this figure, the obtained radiation pattern inside the parabolic chamber and the AUT free space radiation pattern are in good agreement. Table 2 tabulates some types of anechoic chambers for comparison. As can be seen, the nonuniform chamber is the smallest and needs fewer amount of the absorber.

Table 2. Comparison between proposed and reported anechoic chambers, the measuring distance and quiet zone diameter are the same for all chambers and are 1.5 m and 0.5 m, respectively.

Chamber type	Chamber dimensions (m^3)	Area should be covered by absorber (m^2)
Rectangular [5]	$4.5 \times 2.3 \times 2.3$	52
Ellipsoid [9]	$3.7 \times 2.1 \times 2.1$	1.2
Spherical [10]	$4.5 \times 4.5 \times 4.5$	1
Nonuniform	$1.7 \times 1.2 \times 1.2$	0.25

7. CONCLUSIONS

In summary, a new metallic anechoic chamber structure is presented in this paper to greatly decrease the EM absorber usage while obtaining an acceptable quiet zone inside the chamber. The performance of the structure is validated by some numerical examples, and the VSWR method is used to calculate the reflectivity level of the quiet zone in the operating frequency band.

The effects of the chamber shape deformation and surface roughness on the reflectivity level inside the quiet zone are investigated. According to the results, these mechanical imperfections do not cause any serious destructive effect on the chamber performance, and therefore, cheap and simple technologies can be utilized to manufacture the proposed chamber that leads to a low price chamber. Also, to study the effect of the AUT scattered waves on the measurement, a standard horn antenna is placed inside the chamber, and its radiation pattern is obtained by simulation. The results show that the performance of the proposed chamber is certainly acceptable.

REFERENCES

1. Emerson, W. H., "Electromagnetic wave absorbers and anechoic chambers through the years," *IEEE Transactions on Antennas and Propagation*, Vol. 21, No. 4, July 1973.
2. Kineros, C. and V. Ungvichian, "A low cost conversion of semianechoic chamber to fully anechoic chamber for RF antenna measurements," *2003 IEEE International Symposium on Electromagnetic Compatibility*, USA, 2003.
3. Bornkessel, C. and W. Wiesbeck, "Numerical analysis and optimization of anechoic chambers for EMC testing," *IEEE Trans. Electromagn. Compat.*, Vol. 38, No. 3, 499–506, August 1996.
4. Razavi, S. M. J. and M. Khalaj-Amirhosseini, "Optimization an anechoic chamber with ray-tracing and genetic algorithms," *Progress In Electromagnetics Research B*, Vol. 9, 53–68, 2008.
5. Hemming, L. H., *Electromagnetic Anechoic Chambers: A Fundamental Design and Specification Guide*, IEEE Press, 2002.
6. Emerson, W. H., U.S. Patent No. 3,308,463, March 1967, Anechoic Chamber.
7. Hemming, L. H., U.S. Patent No. 4,507,660, March 26, 1985, Anechoic Chamber.
8. Sanchez, G. A., U.S. Patent No. 5,631,661, May 20, 1997, Geometrically Optimized Anechoic Chamber.

9. Razavi, S. M. J., M. Khalaj-Amirhosseini, and A. Cheldavi, "Minimum usage of ferrite tiles in anechoic chambers," *Progress In Electromagnetics Research B*, Vol. 19, 367–383, 2010.

10. Nornikman, H., M. F. B. A. Malek, P. J. Soh, A. A. A.-H. Azremi, F. H. Wee, and A. Hasnain, "Parametric study of pyramidal microwave absorber using rice husk," *Progress In Electromagnetics Research*, Vol. 104, 145–166, 2010.

11. Iqbal, M. N., M. F. B. A. Malek, Y. S. Lee, L. Zahid, M. I. Hussain, M. F. B. Haji Abd Malek, N. F. Mohamed Yusof, N. Saudin, and N. A. Abu Talib, "A simple technique for improving the anechoic performance of a pyramidal absorber," *Progress In Electromagnetics Research M*, Vol. 32, 129–143, 2013.

12. Farahbakhsh, A. and M. Khalaj-amirhosseini, "Using metallic ellipsoid anechoic chamber to reduce the absorber usage," *IEEE Transactions on Antennas and Propagation*, Vol. 63, No. 9, 2015.

13. Farahbakhsh, A. and M. Khalaj-amirhosseini, "Metallic spherical anechoic chamber for antenna pattern measurement," *Chinese Physics B*, Vol. 25, No. 8, 2016.

14. Gielis, J., "A generic geometric transformation that unifies a wide range of natural and abstract shapes," *American Journal of Botany*, Vol. 90, No. 3, 333–338, 2003.

15. Farahbakhsh, A., S. Tavakoli, and A. Seifolhosseini, "Enhancement of genetic algorithm and ant colony optimization techniques using Fuzzy systems," *IEEE International Advance Computing Conference*, March 2009 India.

16. COMSOL Multiphysics®Modeling Software, 2014.

17. Togawa, H., K. Hatakeyama, and K. Yamauchi, "Reflectivity measurements in anechoic chambers in the microwave to millimeter range," *IEEE Transactions on Electromagnetic Compatibility*, Vol. 47, No. 2, 312, 319, May 2005.

18. Appel-Hansen, J., "Reflectivity level of radio anechoic chambers," *IEEE Trans. Antennas Propag.*, Vol. 21, No. 4, 490–498, 1973.

19. Chung, B.-K., C. H. The, and H.-T. Chuah, "Modeling of anechoic chamber using a beam-tracing technique," *Progress In Electromagnetics Research*, Vol. 49, 23–38, 2004.

20. WR-75 Standard Gain Horn Antenna Operates From 10 GHz to 15 GHz with a Normal 10 dB Gain SMA Female Input Connector, Pasternack, Technical Data Sheet, 2013.